CHEMISTRY OF MATERIALS

Perspective

pubs.acs.org/cm

Anisotropic Noble Metal Nanocrystal Growth: The Role of Halides

Samuel E. Lohse,[†] Nathan D. Burrows,[†] Leonardo Scarabelli,[‡] Luis M. Liz-Marzán,*[,‡,§] and Catherine J. Murphy*[,†]

[†]Department of Chemistry, University of Illinois at Urbana−Champaign, 600 S. Mathews Ave., Urbana, Illinois 61801, United States

[‡]BioNanoPlasmonics Laboratory, CIC biomaGUNE, Paseo de Miramón 182, 20009 Donostia-San Sebastián, Gipuzkoa, Spain

[§]Ikerbasque, Basque Foundation for Science, 48011 Bilbao, Biscay, Spain

ABSTRACT: Anisotropic (nonspherical) metal nanoparticles are of widespread research interest because changing the shape of metals at the nanoscale can provide access to materials with unique optical, electronic, and catalytic properties. The development of seeded growth syntheses has provided researchers unprecedented access to anisotropic metal nanocrystals (particularly, gold, silver, platinum, and palladium nanocrystals) with precisely controlled dimensions and crystallographic features. The mechanisms by which the various reagents present in seeded growth syntheses accomplish shape control, however, have yet to be fully elucidated. Recently, the role halide ions play in controlling metal nanocrystal shape has become a subject of particular interest. There are many ways in which the halide ions may direct the anisotropic growth of metal nanocrystals, including modulating the redox potentials of the metal ions, acting as face-specific capping agents, and/or controlling the extent of silver underpotential deposition at the nanocrystal surface. In this Perspective, we examine recent progress in elucidating and articulating the role halide ions play in seeded growth with particular emphasis on gold nanoparticles.

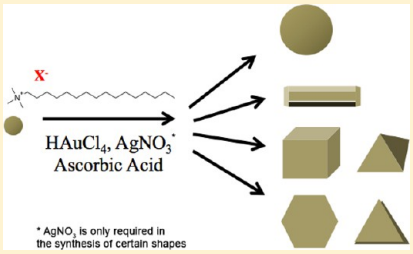

KEYWORDS: *anisotropic noble metal nanoparticles, seeded growth, halides, gold*

INTRODUCTION

Terms such as nanorods, nanowires, nanoprisms, nanostars, etc. have become common within the scientific literature for a wide variety of materials, among which metals occupy a central place.[1−9] The reason behind this is the large influence that nanocrystal morphology has on several physical and chemical properties, including optical[2,4,8] and electronic response[5,7,10] or catalytic activity.[11] Anisotropy offers not only a versatile tool to tune the optical response of gold and silver nanoparticles, through variations in their localized surface plasmon resonances (LSPRs), but also important changes in the electronic conductivity through confinement effects and on the catalytic activity through the availability of high index facets that can facilitate adsorption and surface reactions that are not possible on other surfaces.[1−11]

However, despite the huge volume of literature related to synthesis, characterization, and applications of colloidal anisotropic metal nanoparticles,[1−4,7−12] the mechanisms behind their formation are still under lively debate.[3,8,11−13] Even if the seeded growth method (described in detail below) is accepted as the most efficient one for the synthesis of monodisperse gold nanorods (and other morphologies), it is unclear why growth proceeds along one preferential direction.[3,8] The growth of preformed isotropic nanoparticle seeds into anisotropic nanorods (NRs) requires a symmetry-breaking event, which has not yet been undisputedly disclosed.[3] Since the seeded growth process takes place in a rather complex mixture of salts and surfactants, a variety of mechanisms have been proposed to explain symmetry breaking and anisotropic growth.[8] From a template effect from micellar arrangements of surfactant molecules[8,14] through the selective adsorption of surfactants on certain crystallographic facets,[3] even to the effects of exciting LSPR modes during growth,[15] chemical researchers have invoked a number of parameters as the main reason behind anisotropic growth. Materials scientists favor crystallographic strain as a mechanism to promote anisotropic growth, although how strain arises in colloidal nanoparticles at the atomic level may involve adsorbates, soft structures, etc. It is possible that all of these parameters are somehow involved in the process. It is also clear that the different shapes are characterized by different crystallographic facets, suggesting that these solvent-exposed faces have the lowest surface energy and thereby provide the energetically most favorable morphology.[3,12] However, surface energies are affected not only by the atomic arrangement within the corresponding crystalline lattice (face-centered cubic for these metals) but also by the adsorption of other chemical moieties.[12] In most metal nanoparticle (NP) synthesis methods performed in water or polar solvents, other ions (apart from surfactants and/or polymers) are present. Typically, these ions include halides (mainly chloride, bromide, or iodide).[1−4,6−11] Halide ions have a strong tendency to adsorb on metallic surfaces, and thus, they are likely to affect the corresponding

Special Issue: Celebrating Twenty-Five Years of Chemistry of Materials

Received: July 16, 2013
Revised: September 17, 2013
Published: September 18, 2013

   dx.doi.org/10.1021/cm402384j | *Chem. Mater.* 2014, 26, 34−43

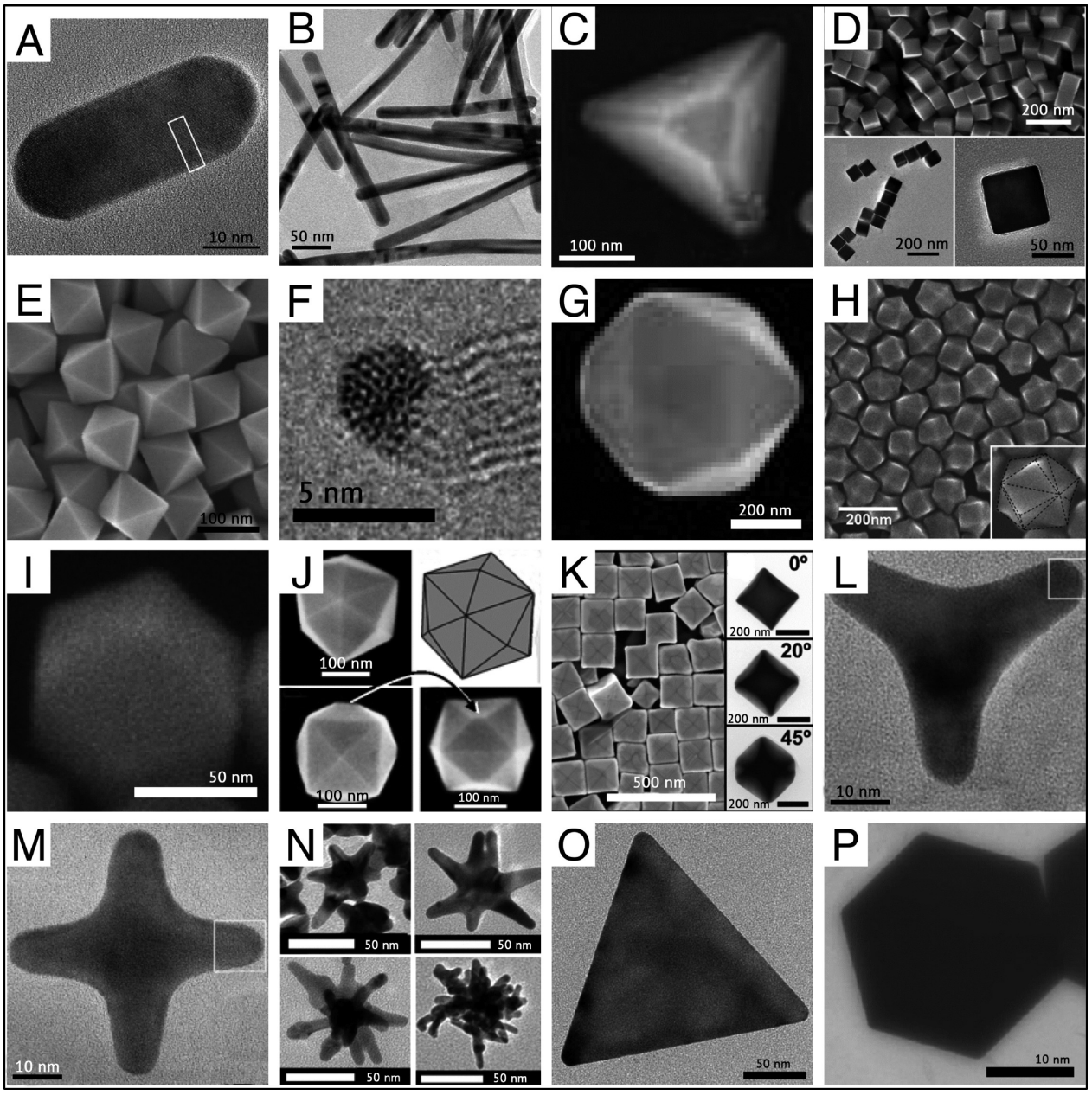

Figure 1. The major classes of noble metal nanoparticle shapes seen through TEM and/or SEM: (A) Au octagonal single-crystal rod, (B) Au pentagonally twinned rods, (C) Au tetrahedron NP, (D) Pd hexahedron (i.e., cube) NPs, (E) Au octahedron NPs, (F) decahedron, (G) Au icosahedron NP, (H) Au trisoctahedron NPs, (I) Au rhombic dodecahedron NP, (J) Pt tetrahexahedron NPs, (K) Au concave hexahedron NPs, (L) Au tripod NP, (M) Au tetrapod NP, (N) Au star NPs, (O) Au triangular plate/prism NP, and (P) Au hexagonal plate/prism NP. Adapted with permission from (A) ref 30, (C and G) ref 25, (D) ref 26, (E) ref 31, (F) ref 32, (H) ref 33, (I) ref 34, (J) ref 35, (K) ref 20, (L and M) ref 36, (N) ref 37, (O) ref 38, and (P) ref 39. Copyright (A and O) 2013 American Chemical Society, (C and G) 2004 WILEY-VCH Verlag GmbH and Co., (D, H, I, K, and P) 2010 American Chemical Society, (E) 2008 American Chemical Society, (F) 2006 WILEY-VCH Verlag GmbH and Co., (J) 2007 American Association for the Advancement of Science, (L and M) 2003 American Chemical Society, and (N) 2012 IOP Publishing.

surface energies.[3,8,12,15] A number of reports have been recently published, regarding the specific use of halides to direct the formation of a certain nanocrystal shape.[12,16−20] For example, bromide is often claimed to be indispensable to obtain well-defined gold nanorods (AuNRs), while iodide has been reported to poison NR formation and induce the formation of nanoplates, as well as various platonic shapes.[12,16−20]

We discuss in this Perspective our views of the effect of halide ions on the anisotropic growth of metal nanocrystals. Although we mainly focus on gold, nanocrystals of silver, platinum, or palladium will also be included, as their formation has also been reported to be strongly influenced by halides.[21−23] We briefly review several examples where halides have been specifically reported to direct anisotropic growth and we discuss whether the presence of halides is strictly necessary for these shapes to occur.

TYPES OF ANISOTROPIC NANOPARTICLE SHAPES

Noble metal nanoparticles (NPs) come in a wide variety of shapes, ranging from the Platonic to branched and irregular nanostructures. Many excellent articles have reviewed the wide variety of shapes (and their nuanced variations) that metal NPs

dx.doi.org/10.1021/cm402384j | Chem. Mater. 2014, 26, 34−43

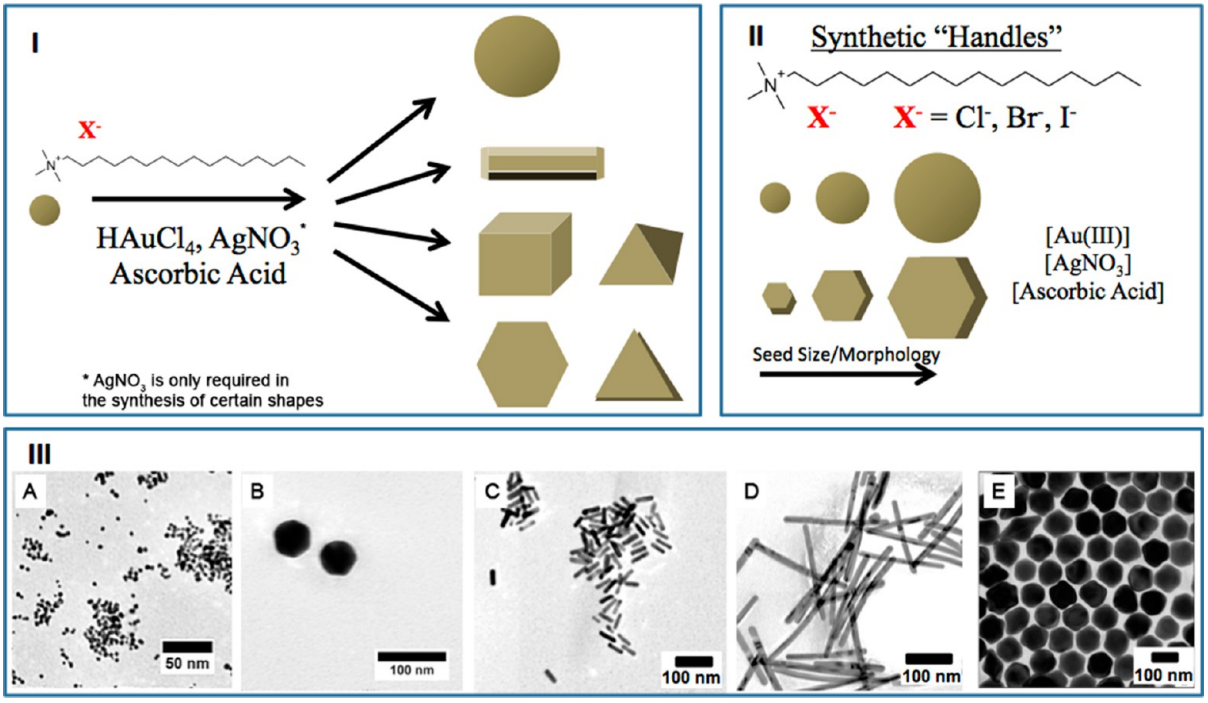

Figure 2. Seeded growth synthesis approaches can be used to prepare a wide variety of gold NP shapes. (I) The general synthetic conditions for a variety of anisotropic AuNPs. (II) A variety of reagent conditions can be altered to change the shape of the product AuNPs in these syntheses, providing a number of synthetic "handles" to control AuNP shape. These include the concentration of the surfactant and the corresponding halide counterion, the size/morphology of the seed, and the concentration of gold salt, silver nitrate, and ascorbic acid. (III) Electron micrographs of various gold nanoparticles: (A) 3.0 nm gold nanospheres, (B) 40.0 nm gold nanospheres, (C) single crystal AuNRs (AR ~3.5), (D) pentagonally twinned gold NRs (AR~15), and (E) trisoctahedral AuNPs.

can have.[3,7,12,24−29] Here, we review the major classes of anisotropic NP shapes and their distinguishing features, a summary of which can be found in Figure 1.

Rods and Wires. The first major class of anisotropic NP shapes comprises one-dimensional structures, namely, rods and wires, where the main difference is the longitudinal length. Rods (and wires) can be a single rectangular or octagonal crystal, a singly twinned crystal, or a 5-fold pentagonal twinned crystal.[13,18,30,40−42] The most common 1D structures are the single crystal octagonal rod/wire (Figure 1A) and the 5-fold twinned pentagonal rod/wire (Figure 1B). Although they are both 1D structures, the direction and exposed crystal faces are quite different between these two rod/wire structures. Single crystal structures are elongated in the ⟨001⟩ direction,[18,43] whereas pentagonally twinned structures are elongated in the ⟨110⟩ direction.[18,42] The pentagonally twinned rods/wires have five lateral facets; however, they are not well-defined as either {100}, {110}, or both.[18,42] The eight lateral facets of single crystal rods/wires were originally thought to be dominated by {100} and {110};[44] however, recent work has demonstrated that the lateral facets are actually higher-index facts (i.e.,{250}) that are beveled at their intersections by {110} facets.[43] On their ends, the 5-fold twinned rods/wires are bound by {111} whereas the single crystal rods/wires are mainly bound by {100} with {110} and {111} facets to round out the ends.[18,30,40,42]

Platonic Shapes. The next class of anisotropic NPs has aspect ratios near one and mainly differ in the number of crystal facets. They are variants of the five platonic shapes (i.e., polyhedrons with the same regular polygon for facets with the same number of polygons meeting at each corner): tetrahedron (4 triangle facets), hexahedron (i.e., cube) (6 square facets), octahedron (8 triangle facets), dodecahedron (12 pentagon facets), and icosahedron (20 triangle facets) (Figure 1C−G).[3,12,13,24−27,32,45] Geometrically, these polyhedrons always have identical polygon facets of their respective number; however, NPs are not nearly so perfect. Their facets are not always the same size or regular polygons and their corners can be truncated resulting in variations such as: {221}-faceted trisoctahedrons, {110}-faceted rhombic dodecahedrons, and even {730}-faceted tetrahexahedrons or {720}-faceted concave hexahedrons (Figure 1H−K).[12,13,24] Generally speaking, tetrahedrons, octahedrons, and icosahedrons are dominated by {111}, whereas hexahedrons are bound by {100} and dodecahedrons by {110}.[25,46]

Branched Nanostructures and Nanoplates. The third class of anisotropic NPs is branched nanostructures (i.e., mono-, bi-, tri-, tetra-, penta-, and multipods; e.g., stars, spike-radiating, and dendritic shapes) (Figure 1L−N).[3,7,27,37,47−51] However, highly branched structures are more difficult to synthesize reproducibly as they are a more complex structure. They are usually polycrystalline with different crystal domains between the core and the branches. Gold branches typically grow in the ⟨110⟩ direction (although other directions have been observed),[7,48,50,51] while platinum branches grow in the ⟨112⟩ direction.[27] The last distinct class of anisotropic NPs comprises two-dimensional structures (i.e., nanoplates, nanoprisms).[3,13,27,38,52] Nanoplates are usually triangular or hexagonal in shape, though truncation is often observed (Figure 1O,P). The surface area of nanoplates is dominated by {111} faces on top and bottom with edges of {211}.

dx.doi.org/10.1021/cm402384j | Chem. Mater. 2014, 26, 34−43

Table 1. Common Seeded Growth Syntheses for Selected Anisotropic Metal Nanoparticles

metal	morphology	reaction condition summary	references
gold	spheres	$HAuCl_4$, CTAB, ascorbic acid, 3.0−12.0 nm seeds	67
	single crystal rods	$HAuCl_4$, $AgNO_3$, CTAB, ascorbic acid, 1.5 nm seeds	68
	twinned rods	$HAuCl_4$, CTAB, ascorbic acid, 3.0 nm seed	59
	dumbbells	$HAuCl_4$, $AgNO_3$, CTAB, ascorbic acid, KI, HCl, 1.5 nm seeds	69
	prisms	$HAuCl_4$, CTAB, NaI, ascorbic acid, 4.0−6.0 nm seeds	70
silver	rods	$AgNO_3$, CTAB, KOH, ascorbic acid, 4.0 nm seeds	71
	plates	$AgNO_3$, CTAB, ascorbic acid	72
platinum	nanowire	K_2PtCl_4, CTAB, $NaBH_4$, water/chloroform	73
	cube	pluronic L64, H_2PtCl_6, H_2	74
palladium	tetrahedra/octahedra	$Pd(acac)_2/Na_2PdCl_4$, polyol, PVP, 5.0 nm seeds	75
	cubes	H_2PdCl_4, CTAB, 40 °C, 22.0 nm Pd seeds	22

SEEDED GROWTH SYNTHESIS FOR ANISOTROPIC SHAPES

Over the past few decades, anisotropic metal nanocrystals (NCs) have been prepared by a variety of synthetic approaches, which have become increasingly convenient while providing ever more precise control over NP shape.[1,3,7,8] The earliest anisotropic metal crystals to be deliberately synthesized were probably nanowires and nanorods (NRs).[8] As early as the 1960s, metal and metal oxide nanowires ("whiskers") were prepared using the vapor−liquid−solid (VLS) approach, a method whose use is still popular today for the synthesis of aligned nanowires.[53,54] By the early 1990s, however, many researchers had turned to electrochemical and photochemical methods for the synthesis of gold and silver NRs/nanowires.[55−58] While these methods were effective for shape control, the resolution and aspect ratio control provided by these approaches was limited, and the synthesis of anisotropic metal crystals was still largely limited to NRs.

In the early 2000s, access to an unprecedented variety of anisotropic metal crystals (including rods, wires, stars, cubes, branched structures, and tetrahedra) became available when a new, convenient chemical synthesis approach, seeded growth in solution, was developed.[1,3,8,49,59,60] The seeded growth approach is a very versatile synthesis, and regardless of what shape of NP is to be synthesized or the identity of the metal core, the seeded growth syntheses of many different anisotropic metal NPs are surprisingly similar.[1,8,14,27] Consequently, what seem like very minor changes in the seeded growth synthesis translate into significant differences in the morphology of the product NPs.[1,8,12,49]

This seeded growth approach involves the synthesis of small metal NP seeds (appearing spherical under electron microscopy), which are then placed in a growth solution containing additional gold monomer and shape-directing agents, and anisotropic growth begins.[49,59,60] In this way, nucleation and growth of the anisotropic crystals are temporally and physically separated, which permits very precise control over NP shape.[1,7,13,49,59−62] The morphology of the final product is governed by a variety of factors, including the size and shape of the seed, the concentration of the capping agents in the growth solution, and the ratio of the metal salt to reductant in the growth solution.[1,3,8,12,27,49] This approach provided, for the first time, a simple, scalable, and relatively high-yield approach to gold and silver NR synthesis, as well as unprecedented aspect ratio control.[1,49,59,60] As a result, the seeded growth approach has become probably the most commonly used synthetic approach for generating anisotropic metal NPs (including gold, silver, platinum, and palladium NPs).[1,8]

Of all the anisotropic metal NPs that can be produced using the seeded growth approach, the synthesis of anisotropic AuNPs has become probably the most extensively studied ones.[1,3,8] The general form of the seeded growth synthesis of anisotropic AuNPs is shown in Figure 2. An initial gold seed is first formed by the reduction of gold salt by sodium borohydride in the presence of a weakly binding ligand such as citrate or cetyltrimethylammonium bromide (CTAB).[1,3,8,49,59,60] A small aliquot of this seed solution is then added to the growth solution, which contains additional gold salt, CTAB, silver nitrate (optional for some NPs, although essential for the growth of single-crystalline gold nanorods), and a weak reducing agent (such as ascorbic acid or hydroquinone).[1,3,8,49,59,60,63] These reagents interact synergistically to direct the shape-controlled growth of the seed. Although AuNPs with a variety of sizes and shapes can be used as seeds, the most common seeds are generally 1.5 nm single-crystalline CTAB-stabilized AuNPs (which appear nearly spherical under an electron microscope but are actually cuboctahedra) or ∼3.0 nm citrate-stabilized AuNPs that are pentagonally twinned.[59,60,64] The seed size and morphology is just one of a number of various reagent conditions that can be tuned to control the final shape of the AuNPs.[1,3,8,49] Other synthetic "handles" that can be utilized to control the shapes of the products include the relative concentrations of gold salt/silver nitrate/ascorbic acid, the concentration of the surfactant, and the CTA^+-halide counterion (Cl^-, Br^-, I^-, Figure 2II).[1,3,8,12,49]

A number of researchers have made excellent use of each of these synthetic "handles" to synthesize anisotropic shapes of increasing complexity using the seeded growth approach.[1,3,8,13,27,60,61] The original demonstrations of seeded growth in 2001 primarily focused on preparing spherical AuNPs of precisely controlled diameter and large aspect ratio AuNRs.[59] By 2004, however, Sau et al. (among others) had demonstrated that a one-step, silver-assisted aqueous seeded growth synthesis (which used CTAB as the capping agent) could be used to prepare a vast number of anisotropic AuNPs, including single-crystalline rods (aspect ratios 1.5−4.0), tetrahedra, cubes, hexagonal plates, and branched structures.[49,59,60] The different shapes could be achieved simply by changing the relative ratios of the seed, silver nitrate concentration, and the ascorbic acid to gold salt ratio.[49] In more recent years, it has also been shown that the same seeded growth approach can be used to more subtly alter AuNR morphology ("overgrowth") or prepare complex nanoparticle morphologies that combine the basic morphology of AuNRs with other shapes.[1,3,8,65,66] In these cases, previously prepared

dx.doi.org/10.1021/cm402384j | Chem. Mater. 2014, 26, 34−43

gold nanorods or platonic shapes (cubes or octahedra) are used as seeds to prepare more complex structures. Some of the more common gold nanoparticle shapes that can be prepared via seeded growth are shown in Figure 2III. The same general seeded growth approach that is used in the synthesis of gold nanoparticles has also been extended to other related metals, such as silver or copper, and even platinum and palladium.[1,3,8,13,61,62] The principal difference among the seeded growth approaches used to prepare these different metal nanocrystals is the composition of the growth solution. While aqueous solutions of halide−surfactant complexes are the standard capping agents in the synthesis of gold and silver nanoparticles, platinum and palladium NPs are more commonly synthesized using seeded growth approaches that occur in polyol solutions, using polymers (such as polyvinylpyrrolidone (PVP)) as capping agents (Table 1); however, Pt/Pd aqueous seeded growth syntheses using surfactants are also known.[62] Accordingly, in discussing the role that halide ions play in directing the growth of anisotropic metal NPs, we will focus the remainder of this review on the seeded growth of AuNPs exclusively.

THE ROLE OF HALIDES IN GOLD NANOPARTICLE SEEDED GROWTH

The mechanism by which the seeded growth approach accomplishes shape control is not yet well understood. Particularly, the importance of the halide anions as a shape-directing agent has only recently begun to be appreciated. Over the past five years, the growth mechanism of anisotropic AuNPs has been the subject of much research (particularly the growth of AuNRs), with the growth of the Au core being studied in detail by a variety of in situ and ex situ methods.[1,6,8,76−78] These studies have revealed a number of important new features regarding the growth mechanism of AuNRs, including the surprising suggestion that AuNRs may grow stochastically, with various fractions of the AuNRs fully forming at different points during the reaction and emerging like popcorn in a microwave.[76] However, a detailed understanding of the chemical processes by which shape control is achieved remains elusive. For instance, the role of silver in these growth processes remains the subject of much debate.[8,14,79] Does the silver ion act in conjunction with the CTAB as a face-specific capping agent?[79] Does preferential silver underpotential deposition (UPD) on specific faces of the growing crystals determine the final morphology of the products?[12,77] Or does the silver influence the structure of the CTAB micelles, providing a soft, rod-shaped template to direct AuNR growth?[14] As difficult as these questions have proven to answer definitively, in the past 3−4 years, a further level of complexity has been added to this mechanistic discussion, as researchers have shown that the identity of the halide counterion also plays a very significant role in determining the morphology of the final products.

Quaternary ammonium surfactants with halide counterions have been an essential part of anisotropic metal nanoparticle synthesis for decades.[3,8] Bromide-surfactant complexes were originally incorporated into the templated electrochemical synthesis of AuNRs, primarily because they were good electrolytes. By the time Jana et al. developed the original three-step seeded growth approach for pentagonally twinned AuNRs, it was suspected that CTAB (which is known to form cylindrical micelles above its second critical micelle concentration) provided a soft template which could direct the anisotropic growth of the AuNRs.[14,59] This view slowly evolved into the hypothesis that CTAB acted as a face-specific capping agent, which would bind preferentially to the longitudinal faces of the developing AuNR, permitting faster reduction of Au atoms at the tips of the rod.[3,8,79] Similar roles for CTAB were proposed in the silver-assisted seeded growth of single-crystalline AuNRs, with the caveat that silver also played a role in either the formation of the cylindrical micelles or the face-specific capping agent was some form of CTA^+−Br^-−Ag^+.[8,79] It has also been proposed that the growth of AuNRs is directed primarily by silver UPD on the longitudinal faces, with CTAB playing a more passive role.[8,12] Between 2007 and 2010, however, several research groups reported that the bromide counterion was more important in directing the growth of AuNRs (particularly in the silver-assisted growth procedure) than the surfactant and that the presence of even relatively small impurities of other halides in the growth solution would completely inhibit AuNR growth.[16,17,76,80] In 2010, for instance, Garg et al. showed that single-crystalline AuNRs of comparable quality and yield could be grown in a growth solution that was only 1.0 mM in CTAB (just above CTAB's first critical micelle concentration) if the total bromide concentration of the solution was kept at 0.09 M or greater.[16] A year later, Bullen et al. studied the effect of bromide concentration on AuNR growth kinetics and found an inverse relationship between the concentration of bromide and the rate of AuNR growth, regardless of whether the bromide was primarily present as CTAB or KBr.[78] Thus, it is clear that the original dependence on CTAB for the synthesis of anisotropic AuNPs was a serendipitous choice, but oddly, it seems that the halide counterion may play a more significant role in controlling AuNP shape than the surfactant.

A variety of researchers have recently come to the same conclusion, demonstrating that changes in the halide counterion (i.e., the use of CTAC or the introduction of KI to the synthesis) can completely change the morphology of the primary product.[12] Several years ago, Smith et al. showed that low concentrations (<3.0 ppm) of iodide impurities present in CTAB would prevent the formation of AuNRs in the silver-assisted synthesis.[18,19] Trace impurities of this kind can be found in reagents offered by many different suppliers, and care should be taken to rigorously check the purity of starting reagents in order to ensure the successful and reproducible synthesis of anisotropic noble nanoparticles. Recently, the deliberate addition of iodide has also been used to alter the morphology of AuNPs produced by the three-step seeded growth synthesis. If the iodide concentration in the CTAB rises above 50 μM, the formation of pentagonally twinned AuNRs is inhibited, and the favored product becomes prisms/nanoplates instead. Several researchers have actually taken advantage of this in recent years to enable the synthesis of new anisotropic shapes (including prisms, trisoctahedra, and other shapes) using growth solutions containing CTAC or a combination of CTAC/I^-.[12] In 2010, Zhang et al. demonstrated that the use of CTAC versus CTAB as the surfactant in a silver assisted seeded growth synthesis could be used to rationally control the shape of the products, under otherwise identical synthesis conditions. In this case, the use of CTAB led to the formation of tetrahexahedra, while the use of CTAC promoted the formation of concave cubes.[20] Two years later, Mirkin et al. extended this study to show that the ratio of silver nitrate to halide and the selection of the appropriate halide counterion could be used to rationally prepare a variety of anisotropic AuNPs.[12] These studies indicate that specific halides will lead to

dx.doi.org/10.1021/cm402384j | Chem. Mater. 2014, 26, 34−43

the preferential formation of different anisotropic shapes (Figure 3), under otherwise identical seeded growth conditions.

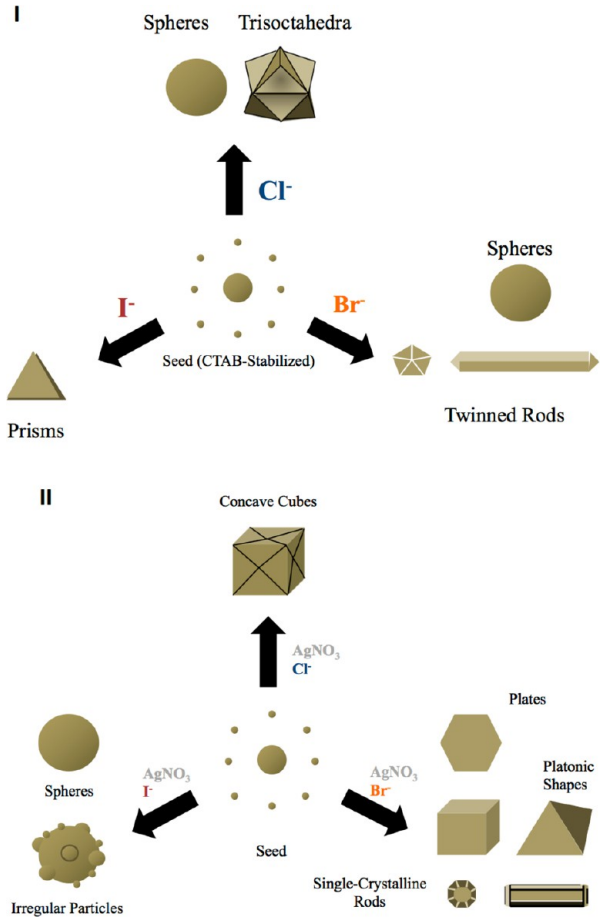

Figure 3. The identity of the halide used in AuNP seeded growth synthesis has a strong influence on AuNP morphology; some anisotropic shapes can only be produced when the synthetic conditions include high concentrations of a specific halide. (I) AuNP shapes typically formed using each halide in the absence of silver nitrate. (II) In the presence of silver nitrate, the different halide ions favor the formation of distinctly different shapes. The shapes shown here are "typical" shapes achieved with each halide; however, some shapes can be prepared in the presence of more than one halide ion, if the other growth conditions are altered.

As a result, it is clear that the nature of the halide counterion plays a crucial role in the growth processes of anisotropic AuNPs, but it is not yet clear which potential halide–metal interactions are primarily responsible for shape control.

Completely understanding the role of the halide in the synthesis of anisotropic NPs is challenging, because there are many different halide–metal crystal and halide–metal ion interactions (and these interactions may compete with each other or act synergistically to effect shape control) that need to be accounted for in a seeded growth synthesis. Primarily, until last year, researchers have focused on the potential for halides to act as face-specific capping agents (a single type of metal crystal–halide interaction). However, there are many possible roles that halides could play in the synthesis of anisotropic AuNPs. Potential X^-–metal interactions fall into three broad categories: halide interactions with the growing metal crystal, halide interactions with ionic gold, and interactions with the ancillary reagents (e.g., silver nitrate). More specifically, these interactions may include: the ability of the halide to change the reduction potential of either Au(III) or Au(I) prior to the addition of the seed, preferential halide binding to different gold crystal faces, the influence of the halide concentration on the shape of the CTA^+X^- micelle, and the effect of the halide on silver underpotential deposition, among others. Investigating any of these potential scenarios is challenging in a reaction mixture as complex as the milieu in which seeded growth occurs, and deciding whether a particular halide in a particular synthesis (e.g., bromide in the silver-assisted synthesis of AuNRs) exerts shape control primarily through one of these roles or a combination of several different roles is even more challenging. Nevertheless, in the past few years, several researchers have made significant strides in better articulating the often-complex roles of halides in anisotropic AuNP synthesis.

Recently, Mirkin et al. investigated the role of halides, silver concentration, and growth rate on the final shape of AuNPs (Figure 4).[12] They found that halides primarily serve three roles during the synthesis of the specific shapes they investigated (which included tris-octahedra, concave cubes, prisms, and tetrahedra, but not AuNRs): (1) the halides modulate the reduction potential of ionic gold prior to seed addition (Figure 4A), (2) the halides passivate the AuNP surface (Figure 4A), and (3) in the silver-assisted syntheses, the halides also modulate the extent of silver UPD (Figure 4B,C). The UPD process is affected by both Ag^+ concentration (Figure 4B) and the presence of halides (Figure 4C). It is important to remember that many of their observations, while of crucial importance, are particular to certain solution conditions and it is not yet clear whether their results can be fully generalized to other syntheses.

Mirkin et al. found that in the absence of silver, larger halides (e.g., I^-) encourage slower AuNP growth by altering the reduction potential of $[AuX_2]^-$ and by directly passivating the facets of the growing crystal, which correlates with the formation of AuNPs with lower surface energy faces.[12] In the presence of silver, however, they conclude that the halides primarily exert shape control by controlling the rate/stability of Ag UPD (affecting the mobility of silver atoms), and the manner of this control depends on the concentration of halides in solution following the trend of the interaction of Au and Ag with the different halides: Ag UPD–Cl > Ag UPD–Br > Ag UPD–I and Au–I > Au–Br > Au–Cl. When larger halides are only present in trace amounts, the stability of the Ag UPD layer is somewhat decreased, leading to the formation of shapes with higher-energy facets. However, when I^- or Br^- are present in high concentration, they prevent silver deposition on the particle surface, and this limits the number of shapes that can be generated.[12] They suggested that this concept allows a precise control over the growth rate and the surface chemistry, through a tight control over the concentrations of silver and halides.

NEW DEVELOPMENTS: DO HALIDES REALLY MATTER?

Although we have seen in the previous sections that halides appear to be essential for anisotropic growth, recent literature reports provide evidences that are in conflict with this concept. However, it should be noted that the conclusions are often contradictory and we therefore include a discussion here. For example, DuChen et al. systematically studied the effect of Cl^-, Br^-, and I^- on the growth of citrate seeds both using CTAB and CTAC as surfactants.[38] The main conclusions are that Cl^-

dx.doi.org/10.1021/cm402384j | Chem. Mater. 2014, 26, 34–43

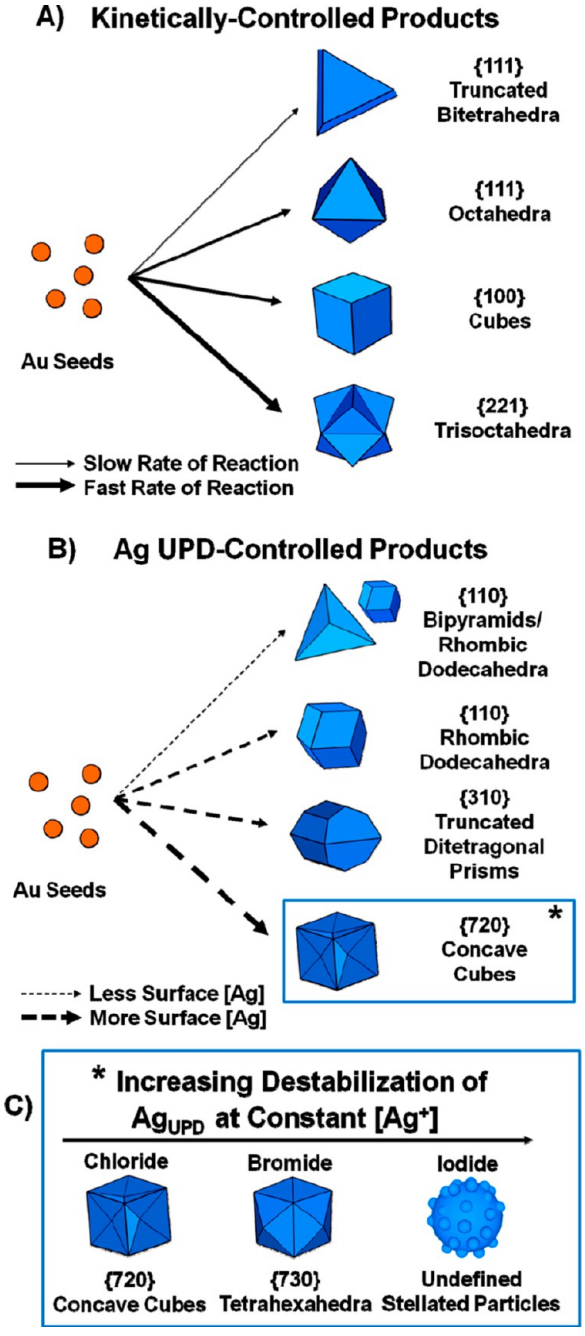

Figure 4. Scheme illustrating the six rules proposed by Mirkin. Halides and silver ions can be used to direct the growth of gold seeds down different growth pathways to yield different shaped products: (A) kinetically-controlled products in the absence of silver ions; (B) Ag underpotential deposition-controlled products where the interactions of silver with the particle surface dictate product shape; C) effect of varying the stability of the AgUPD layer with high concentrations of chloride, bromide, or iodide in the growth solution, yielding concave cubes, tetrahexahedra, and stellated particles, respectively. Adapted from ref. 12. Copyright 2012 American Chemical Society.

is unable to produce well-defined anisotropic architectures, while Br^- allows the system to evolve toward rod shape and the presence of I^- leads to the development of nanoprisms and hexagonal nanoplate morphologies. The authors proposed that passivation of low-index Au facets occurs because of adsorption of the different halides, with a strength that follows the order of $Cl^- < Br^- < I^-$, which is likely to arise from the different redox

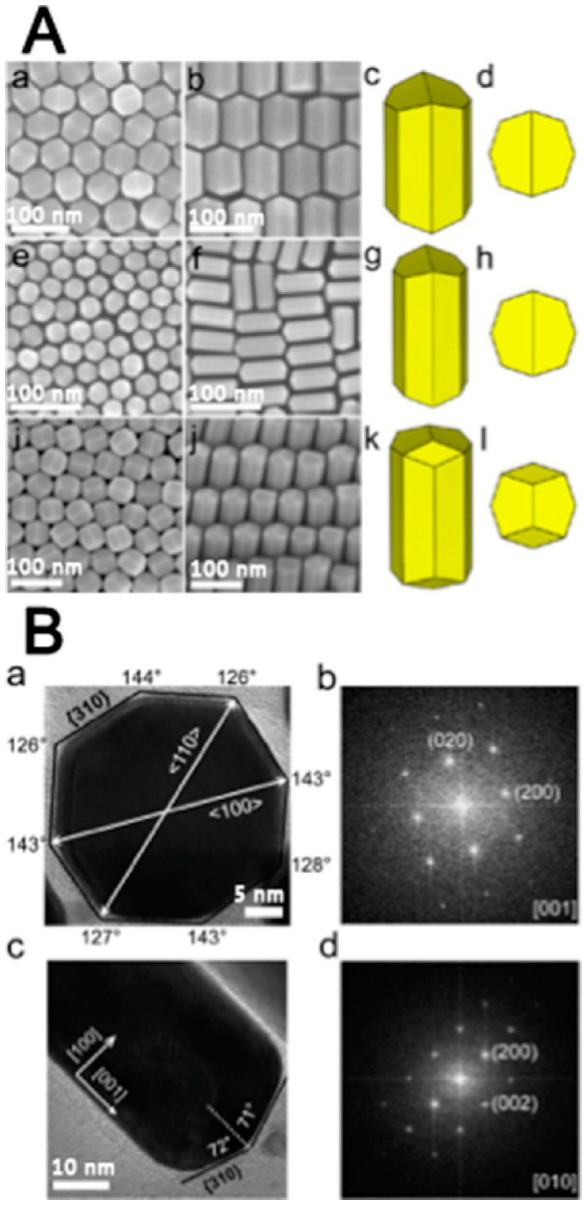

Figure 5. Summary of Murray's bromide-free synthesis. (A) SEM images of vertically aligned (a,e,i), horizontally aligned (b,f,j) and structural models (c,d,g,h,k,l) showing the morphology of Au NRs synthesized in different conditions. (B) HRTEM image (a,c) and corresponding FFT pattern demonstrating the [001] zone axis. The white arrows show the ⟨100⟩ and ⟨110⟩ crystallographic directions calculated by FFT. Adapted from ref 89. Copyright 2013 American Chemical Society.

potentials of the Au precursor in the presence of the different halide ligands, but no consideration was taken of the rates of reduction or growth. A completely opposite approach was taken by Huang and Chiu, who underlined that passivation of the surface of growing Au NPs cannot explain the real mechanism of action of the halides, while the main contribution must be attributed to the different reduction and growth rates.[24] This claim was based on a systematic study of the growth of CTAC-capped seeds under different conditions (including silver-assisted and silver-free protocols), showing that it is possible to obtain a wide range of crystallographic habits by simply modulating the reaction rates involved in the synthesis. In particular, a faster growth rate leads to

dx.doi.org/10.1021/cm402384j | Chem. Mater. 2014, 26, 34−43

crystallographic habits characterized by higher index facets. However, this mechanism would not explain why the effect of halides significantly changes when Ag^+ ions are present. A combination of reaction kinetics and halide adsorption was recently claimed to determine reshaping upon Ag coating, which was supported by density functional theory (DFT) calculations.[81] Nonetheless, Xiao and Qi provided an overview of different gold nanocrystal syntheses where size, shape, and crystal habit are determined by the use of different surfactants, without taking into consideration the role of the halide counterions.[41]

To obtain a more complete picture, we should also take into consideration synthesis methods involving the use of halide-free solvents and capping agents. This is often the case in the so-called polyol methods, where ethylene glycol or a higher polyol act as both solvent and reducing agent, almost invariably in the presence of polyvinylpyrrolidone (PVP) as a capping polymer.[25,28,31] In these procedures, it should be noted that the redox potential of PVP changes with temperature, which can be exploited to precisely control the reduction rate, ultimately controlling the final morphologies of the NPs. Similar observations were made when dimethylformamide (DMF) was used instead of the polyols,[82] where variation of the reaction conditions (PVP and metal salt concentrations, temperature, or presence of seeds) was found to lead to NPs with different morphologies.[46,47] Although these syntheses do not involve the use of halide-containing surfactants, it should be noted that the gold precursor has always been $HAuCl_4$, and therefore, the growth conditions are never halide-free. Additionally, when discussing the adsorption of halides on the particles surface, it must be kept in mind that the solvents have chemical and physical properties very different from water, as well as the capping strength of PVP, which cannot be compared with that of surfactants like CTAB. While halides have often been considered as spectator ions in these syntheses, Xia and co-workers have extensively discussed other effects, such as the role of chloride as an etchant for removal of twin planes.[50,83]

As discussed in the previous section, Mirkin et al. recently presented an excellent study on the halides effects in both the presence and absence of Ag. Despite the attempt of this paper to provide a global view of the "halide problem", the observations cannot be completely generalized because the study refers exclusively to the use of CTAC-capped seeds, which are significantly larger (7 or 40 nm) as compared to both CTAB (<2 nm) and citrate seeds (3.5−5 nm) and, therefore, most likely present a different surface chemistry. An important consideration when dealing with the role of halides in AuNP synthesis is the discrimination between thermodynamic and kinetic products. Kinetic considerations indicate that better-defined NPs are generally formed when the growth rate is slower (thereby allowing the system to reach the thermodynamic minimum energy, i.e., the thermodynamic product) while the NPs are usually less anisotropic (AR < 1.5). However, kinetic products are typically characterized by fast growth and high anisotropy (AR ≫ 2). It is interesting to note that, in the later case, halides do not seem to have a clear effect on the process. For example, Pallavicini et al. proposed the synthesis of branched Au NPs using a zwitterionic surfactant without the addition of heavy halides like Br^- or I^-.[48,84] The same observation can be found in a totally different system like the surfactant-free nanostars reported by Yuan et al.[37] Both synthetic routes are silver-assisted, and the presence of Ag^+ is a key parameter to obtain the necessary symmetry break. A detailed study of the ability of silver to produce anisotropic NPs is beyond the scope of this Perspective, but it is worth mentioning that the synthesis of Au nanostars using the DMF/PVP system is both bromide-free and silver-free.[47]

The important message here is that it is essential to distinguish between the stabilization of certain facets to direct the synthesis toward a precise crystallographic habit and breaking the face-centered cubic symmetry to achieve anisotropic NPs. This discrimination is not always clear in the literature and can give rise to misunderstandings. Interestingly, both thermodynamic and kinetic effects affect the synthesis of AuNRs. Although the aspect ratio can be readily tuned between 2 and 5, high quality products require the growth rate to be slow (typically >4 h). Additionally, the synthesis is strongly affected by the presence of halides, such that a certain amount of bromide is a prerequisite, while the growth is extremely sensitive to the presence of iodide or other impurities.[18,19] It is entirely possible that the reason certain experiments have not agreed on the role of halides is that minute amounts of halide impurities may be present in stock reagents (or even nanopure water sources). Currently, it is still rare for nanomaterials researchers to independently characterize the purity of their starting materials, but it is essential to work with analytically pure starting materials (or at least starting materials with well-documented impurity profiles) when attempting mechanistic studies. This is particularly true for the study of complex chemical reactions, such as the growth of metal nanocrystals. We would recommend that researchers working to understand the growth of metal nanocrystals thoroughly check the purity of their reagents and starting materials (and even products) using sensitive elemental analysis techniques (e.g., ICP-MS) prior to beginning experiments.

In a recent addition to the optimization of AuNR synthesis, Ye et al. achieved a significant improvement by using a binary surfactant mixture of CTAB and sodium oleate (NaOL), as well as aromatic additives, which gave them access to nanorods within a wide size range and improved monodispersity.[85,86] The rationale behind the effect of oleic acid seems to be the hydrophobic interaction between the tails and the head groups (Coulomb interactions with the deprotonated carboxylic acid moiety) of both surfactants. These interactions allow surfactant molecules to stay closer to one another, with a higher degree of control on the growth reaction. However, there are some curious features of the possible mechanism for AuNR formation.

The assumption of a significant deprotonation of the acidic moiety is in contrast with the strongly acidic conditions (pH 0.95). The pK_a of oleic acid is 9.85,[87] and even taking into consideration a possible change in acidity due to the interaction with the surface of the AuNRs as reported by Wang et al.,[88] a significant deprotonation seems unlikely. Notably, the proposed protocol presents important differences from other syntheses, such as the significant increase in the Ag/Au molar ratio (up to 3-fold) and the use of an extremely small amount of seed solution (up to 120 times less). These two observations alone might explain the increased dimensions (due to the small amount of seeds), the stabilization of different high-index facets, and the increased resistance (10 times) to iodide contamination (both thanks to the higher silver concentration, see above). More recently, the same authors also demonstrated that this system allows the synthesis of high-quality Au NRs even when CTAB is fully replaced by a mixture of CTAC and NaOL (Figure 5).[89] Unfortunately, the conditions are not completely

dx.doi.org/10.1021/cm402384j | Chem. Mater. 2014, 26, 34−43

bromide-free, since the seeds were still prepared using the standard CTAB protocol, for a final bromide concentration of 0.25 mM, i.e., half the concentration of Au. Thus, the "bromide-free" synthesis is not yet truly bromide-free.

CLOSING REMARKS

Clearly, the multiple possible roles of halide counterions in anisotropic metal nanoparticle synthesis have all been invoked at one time or another: redox modifier, adsorbate, complexing agent (with silver), and surfactant micelle controller. The tendency of the chemist is to think that only one of these is the right one or at least the main one, but this too is an assumption. For instance, Alivisatos et al. have shown that the growth of platinum nanocrystals, by single particle imaging in a wet TEM cell, can produce apparently the same products by two completely different pathways (monomer addition versus small particle coalescence).[90] In addition to standard surface characterization techniques such as X-ray photoelectron spectroscopy or vibrational spectroscopy (both of which support the notion of chemisorbed bromide on Au NRs), studies in which individual nanoparticle growth is observed in real time, with atomic-level elemental analysis capability in colloidal solution, would be most valuable in elucidating mechanistic pathways. We anxiously await such capability.

AUTHOR INFORMATION

Corresponding Authors

*E-mail: llizmarzan@cicbiomagune.es.
*E-mail: murphycj@illinois.edu.

Notes

The authors declare no competing financial interest.

Biographies

Samuel E. Lohse is a postdoctoral researcher in Catherine Murphy's group at the University of Illinois at Urbana−Champaign. He received his Ph.D. from the University of Oregon's Chemistry Department in 2011, after completing his undergraduate studies in Chemistry and Biochemistry at Idaho State University.

Nathan D. Burrows is currently a postdoctoral research associate in Catherine J. Murphy's research group at the University of Illinois at Urbana−Champaign. He received his Ph. D. (2013) and M.S. (2009) emphasizing in Materials Chemistry from the University of Minnesota in Minneapolis after completing his B.A. (2007) at Concordia University in St. Paul, MN with a major emphasis in chemistry and minor emphasis in theatre.

Leonardo Scarabelli received his bachelor and master degrees in Chemistry from the University of Pavia (Italy) with a thesis work entitled "Monolayers of gold nanostars on glass: antibacterial and phototermic effect". He is currently working on his Ph.D. at CICbiomaGUNE in San Sebastián, under the supervision of Luis M. Liz-Marzán. His research focuses on the synthesis and directed self-assembly of metal nanoparticles of different shapes and sizes for the fabrication of biosensors.

Luis M. Liz-Marzán has a Ph.D. from the University of Santiago de Compostela (1992) and was a postdoc at Utrecht University and visiting professor at various universities and research centers. After holding a chair in Physical Chemistry at the University of Vigo (1995−2012), he is currently an Ikerbasque Research Professor and Scientific Director of CIC biomaGUNE in San Sebastián. His current interests include nanoparticle synthesis and assembly, nanoplasmonics, and nanoparticle-based sensing and diagnostic tools.

Catherine J. Murphy is the Peter C. and Gretchen Miller Markunas Professor of Chemistry at the University of Illinois at Urbana−Champaign (UIUC). She earned two B.S. degrees, one in chemistry and one in biochemistry, from UIUC in 1986. She was awarded her Ph.D. from the University of Wisconsin, Madison, in 1990, under the direction of A. B. Ellis. From 1990 to 1993, she held consecutive national postdoctoral fellowships (NSF, then NIH) at the California Institute of Technology, working in the laboratory of J. K. Barton. In 1993, she began her independent academic career at the University of South Carolina. After rising through the ranks at South Carolina, she was recruited back to UIUC in 2009, where she directs a research laboratory focused on the synthesis, functionalization, applications, and implications of inorganic nanomaterials.

ACKNOWLEDGMENTS

S.E.L. and C.J.M. thank the National Science Foundation's Center for Sustainable Nanotechnology (CHE-1240151) for support. N.D.B. and C.J.M. thank DARPA (HR0011-13-2-002) for support. L.M.L.-M. acknowledges funding from the European Science Foundation (ERC Advanced Grant #267867, Plasmaquo).

REFERENCES

(1) Dreaden, E. C.; Alkilany, A. M.; Huang, X.; Murphy, C. J.; El-Sayed, M. A. *Chem. Soc. Rev.* **2012**, *41*, 2740.
(2) Eustis, S.; El-Sayed, M. A. *Chem. Soc. Rev.* **2006**, *35*, 209.
(3) Grzelczak, M.; Perez-Juste, J.; Mulvaney, P.; Liz-Marzan, L. M. *Chem. Soc. Rev.* **2008**, *37*, 1783.
(4) Kennedy, L. C.; Bickford, L. R.; Lewinski, N. A.; Coughlin, A. J.; Hu, Y.; Day, E. S.; West, J. L.; Drezek, R. A. *Small* **2010**, *7*, 169−183.
(5) Kumar, S.; Nann, T. *Small* **2006**, *2*, 316−329.
(6) Langille, M. R.; Zhang, J.; Personick, M. L.; Li, S.; Mirkin, C. A. *Science* **2012**, *337*, 954−957.
(7) Lim, B.; Xia, Y. *Angew. Chem., Int. Ed.* **2010**, *50*, 76−85.
(8) Lohse, S. E.; Murphy, C. J. *Chem. Mater.* **2013**, *25*, 1250−1261.
(9) Tao, A. R.; Habas, S.; Yang, P. *Small* **2008**, *4*, 310−325.
(10) Sardar, R.; Funston, A. M.; Mulvaney, P.; Murray, R. W. *Langmuir* **2009**, *25*, 13840−13851.
(11) Zhang, H.; Jin, M.; Xiong, Y.; Lim, B.; Xia, Y. *Acc. Chem. Res.* **2013**, *46*, 1783−1794.
(12) Langille, M. R.; Personick, M. L.; Zhang, J.; Mirkin, C. A. *J. Am. Chem. Soc.* **2012**, *134*, 14542−14554.
(13) Xia, Y.; Xiong, Y.; Lim, B.; Skrabalak, S. E. *Angew. Chem., Int. Ed.* **2008**, *48*, 60−103.
(14) Jana, N. R. *Small* **2005**, *1*, 875−882.
(15) Jin, R.; Cao, Y. C.; Hao, E.; Métraux, G. S.; Schatz, G. C.; Mirkin, C. A. *Nature* **2003**, *425*, 487−490.
(16) Garg, N.; Scholl, C.; Mohanty, A.; Jin, R. *Langmuir* **2010**, *26*, 10271−10276.
(17) Si, S.; Leduc, C.; Delville, M.-H.; Lounis, B. *ChemPhysChem* **2012**, *13*, 193−202.
(18) Smith, D. K.; Miller, N. R.; Korgel, B. A. *Langmuir* **2009**, *25*, 9518−9524.
(19) Smith, D. K.; Korgel, B. A. *Langmuir* **2008**, *24*, 644−649.
(20) Zhang, J.; Langille, M. R.; Personick, M. L.; Zhang, K.; Li, S.; Mirkin, C. A. *J. Am. Chem. Soc.* **2010**, *132*, 14012−14014.
(21) Wang, F.; Li, C.; Sun, L.-D.; Wu, H.; Ming, T.; Wang, J.; Yu, J. C.; Yan, C.-H. *J. Am. Chem. Soc.* **2011**, *133*, 1106−1111.
(22) Niu, W.; Li, Z.-Y.; Shi, L.; Liu, X.; Li, H.; Han, S.; Chen, J.; Xu, G. *Cryst. Growth Des.* **2008**, *8*, 4440−4444.
(23) Habas, S. E.; Lee, H.; Radmilovic, V.; Somorjai, G. A.; Yang, P. *Nat. Mater.* **2007**, *6*, 692−697.
(24) Huang, M. H.; Chiu, C.-Y. *J. Mater. Chem. A* **2013**, *1*, 8081−8092.
(25) Kim, F.; Connor, S.; Song, H.; Kuykendall, T.; Yang, P. *Angew. Chem., Int. Ed.* **2004**, *43*, 3673−3677.

(26) Niu, W.; Zhang, L.; Xu, G. *ACS Nano* **2010**, *4*, 1987−1996.
(27) Sau, T. K.; Rogach, A. L. *Adv. Mater.* **2010**, *22*, 1781−1804.
(28) Wiley, B.; Sun, Y.; Mayers, B.; Xia, Y. *Chem.−Eur. J.* **2005**, *11*, 454−463.
(29) Quan, Z.; Wang, Y.; Fang, J. *Acc. Chem. Res.* **2013**, *46*, 191−202.
(30) Park, K.; Drummy, L. F.; Wadams, R. C.; Koerner, H.; Nepal, D.; Fabris, L.; Vaia, R. A. *Chem. Mater.* **2013**, *25*, 555−563.
(31) Li, C.; Shuford, K. L.; Chen, M.; Lee, E. J.; Cho, S. O. *ACS Nano* **2008**, *2*, 1760−1769.
(32) Montejano-Carrizales, J. M.; Rodríguez-López, J. L.; Pal, U.; Miki-Yoshida, M.; Jose-Yacaman, M. *Small* **2006**, *2*, 351−355.
(33) Yu, Y.; Zhang, Q.; Lu, X.; Lee, J. Y. *J. Phys. Chem. C* **2010**, *114*, 11119−11126.
(34) Wu, H.-L.; Kuo, C.-H.; Huang, M. H. *Langmuir* **2010**, *26*, 12307−12313.
(35) Tian, N.; Zhou, Z. Y.; Sun, S. G.; Ding, Y.; Wang, Z. L. *Science* **2007**, *316*, 732−735.
(36) Chen, S.; Wang, Z. L.; Ballato, J.; Foulger, S. H.; Carroll, D. L. *J. Am. Chem. Soc.* **2003**, *125*, 16186−16187.
(37) Yuan, H.; Khoury, C. G.; Hwang, H.; Wilson, C. M.; Grant, G. A.; Vo-Dinh, T. *Nanotechnology* **2012**, *23*, 075102.
(38) DuChene, J. S.; Niu, W.; Abendroth, J. M.; Sun, Q.; Zhao, W.; Huo, F.; Wei, W. D. *Chem. Mater.* **2013**, *25*, 1392−1399.
(39) Lin, G.; Lu, W.; Cui, W.; Jiang, L. *Cryst. Growth Des.* **2010**, *10*, 1118−1123.
(40) Murphy, C. J.; Thompson, L. B.; Chernak, D. J.; Yang, J. A.; Sivapalan, S. T.; Boulos, S. P.; Huang, J.; Alkilany, A. M.; Sisco, P. N. *Curr. Opin. Colloid Interface Sci.* **2011**, *16*, 128−134.
(41) Xiao, J.; Qi, L. *Nanoscale* **2011**, *3*, 1383.
(42) Murphy, C. J.; Sau, T. K.; Gole, A. M.; Orendorff, C. J.; Gao, J.; Gou, L.; Hunyadi, S. E.; Li, T. *J. Phys. Chem. B* **2005**, *109*, 13857−13870.
(43) Carbo-Argibay, E.; Rodríguez-González, B.; Gomez-Grana, S.; Guerrero-Martinez, A.; Pastoriza-Santos, I.; Perez-Juste, J.; Liz-Marzan, L. M. *Angew. Chem., Int. Ed.* **2010**, *49*, 9397−9400.
(44) Wang, Z. L.; Mohamed, M. B.; Link, S.; El-Sayed, M. A. *Surf. Sci.* **1999**, *440*, L809−L814.
(45) Rao, C. N. R.; Ramakrishna Matte, H. S. S.; Voggu, R.; Govindaraj, A. *Dalton Trans.* **2012**, *41*, 5089.
(46) Sánchez-Iglesias, A.; Pastoriza-Santos, I.; Pérez-Juste, J.; Rodríguez-González, B.; García de Abajo, F. J.; Liz-Marzán, L. M. *Adv. Mater.* **2006**, *18*, 2529−2534.
(47) Kumar, P. S.; Pastoriza-Santos, I.; Rodríguez-González, B.; de Abajo, F. J. G.; Liz-Marzan, L. M. *Nanotechnology* **2008**, *19*, 015606.
(48) Pallavicini, P.; Chirico, G.; Collini, M.; Dacarro, G.; Donà, A.; D'Alfonso, L.; Falqui, A.; Diaz-Fernandez, Y.; Freddi, S.; Garofalo, B.; Genovese, A.; Sironi, L.; Taglietti, A. *Chem. Commun.* **2011**, *47*, 1315.
(49) Sau, T. K.; Murphy, C. J. *J. Am. Chem. Soc.* **2004**, *126*, 8648−8649.
(50) Zhang, H.; Xia, X.; Li, W.; Zeng, J.; Dai, Y.; Yang, D.; Xia, Y. *Angew. Chem., Int. Ed.* **2010**, *49*, 5296−5300.
(51) Guerrero-Martinez, A.; Barbosa, S.; Pastoriza-Santos, I.; Liz-Marzan, L. M. *Curr. Opin. Colloid Interface Sci.* **2011**, *16*, 118−127.
(52) Straney, P. J.; Andolina, C. M.; Millstone, J. E. *Langmuir* **2013**, *29*, 4396−4403.
(53) Wagner, R. S.; Ellis, W. C. *Appl. Phys. Lett.* **1964**, *4*, 89−90.
(54) Ito, D.; Jespersen, M. L.; Hutchison, J. E. *ACS Nano* **2008**, *2*, 2001−2006.
(55) Yu, Y.-Y.; Chang, S.-S.; Lee, C.-L.; Wang, C. C. *J. Phys. Chem. B* **1997**, *101*, 6661−6664.
(56) Link, S.; Wang, Z. L.; El-Sayed, M. A. *J. Phys. Chem. B* **2000**, *104*, 7867−7870.
(57) Kim, F.; Song, J. H.; Yang, P. *J. Am. Chem. Soc.* **2002**, *124*, 14316−14317.
(58) Esumi, K.; Matsuhisa, K.; Torigoe, K. *Langmuir* **1995**, *11*, 3285−3287.
(59) Jana, N. R.; Gearheart, L.; Murphy, C. J. *Adv. Mater.* **2001**, *13*, 1389−1393.
(60) Nikoobakht, B.; El-Sayed, M. A. *Chem. Mater.* **2003**, *15*, 1957−1962.
(61) Liz-Marzan, L. M. *Chem. Commun.* **2013**, *49*, 16−18.
(62) Xiong, Y.; Xia, Y. *Adv. Mater.* **2007**, *19*, 3385−3391.
(63) Vigderman, L.; Zubarev, E. R. *Chem. Mater.* **2013**, *25*, 1450−1457.
(64) Liu, M.; Guyot-Sionnest, P. *J. Phys. Chem. B* **2005**, *109*, 22192−22200.
(65) Gou, L.; Murphy, C. J. *Chem. Mater.* **2005**, *17*, 3668−3672.
(66) Sohn, K.; Kim, F.; Pradel, K. C.; Wu, J.; Peng, Y.; Zhou, F.; Huang, J. *ACS Nano* **2009**, *3*, 2191−2198.
(67) Jana, N. R.; Gearheart, L.; Murphy, C. J. *Langmuir* **2001**, *17*, 6782−6786.
(68) Sau, T. K.; Murphy, C. J. *Langmuir* **2004**, *20*, 6414−6420.
(69) Grzelczak, M.; Sánchez-Iglesias, A.; Rodríguez-González, B.; Alvarez-Puebla, R.; Perez-Juste, J.; Liz-Marzan, L. M. *Adv. Funct. Mater.* **2008**, *18*, 3780−3786.
(70) Millstone, J. E.; Wei, W.; Jones, M. R.; Yoo, H.; Mirkin, C. A. *Nano Lett.* **2008**, *8*, 2526−2529.
(71) Jana, N. R.; Gearheart, L.; Murphy, C. J. *Chem. Commun.* **2001**, 617−618.
(72) Chen, S.; Carroll, D. L. *Nano Lett.* **2002**, *2*, 1003−1007.
(73) Song, Y.; Garcia, R. M.; Dorin, R. M.; Wang, H.; Qiu, Y.; Coker, E. N.; Steen, W. A.; Miller, J. E.; Shelnutt, J. A. *Nano Lett.* **2007**, *7*, 3650−3655.
(74) Niesz, K.; Grass, M.; Somorjai, G. A. *Nano Lett.* **2005**, *5*, 2238−2240.
(75) Lim, B.; Jiang, M.; Tao, J.; Camargo, P. H. C.; Zhu, Y.; Xia, Y. *Adv. Funct. Mater.* **2009**, *19*, 189−200.
(76) Edgar, J. A.; McDonagh, A. M.; Cortie, M. B. *ACS Nano* **2012**, *6*, 1116−1125.
(77) Personick, M. L.; Langille, M. R.; Zhang, J.; Mirkin, C. A. *Nano Lett.* **2011**, *11*, 3394−3398.
(78) Bullen, C.; Zijlstra, P.; Bakker, E.; Gu, M.; Raston, C. *Cryst. Growth Des.* **2011**, *11*, 3375−3380.
(79) Hubert, F.; Testard, F.; Spalla, O. *Langmuir* **2008**, *24*, 9219−9222.
(80) Sau, T. K.; Murphy, C. J. *Philos. Mag.* **2007**, *87*, 2143−2158.
(81) Gomez-Grana, S.; Goris, B.; Altantzis, T.; Fernández-López, C.; Carbo-Argibay, E.; Guerrero-Martinez, A.; Almora-Barrios, N.; Lopez, N.; Pastoriza-Santos, I.; Perez-Juste, J.; Bals, S.; Van Tendeloo, G.; Liz-Marzan, L. M. *J. Phys. Chem. Lett.* **2013**, *4*, 2209−2216.
(82) Pastoriza-Santos, I.; Liz-Marzan, L. M. *Adv. Funct. Mater.* **2009**, *19*, 679−688.
(83) Wiley, B.; Herricks, T.; Sun, Y.; Xia, Y. *Nano Lett.* **2004**, *4*, 1733−1739.
(84) Casu, A.; Cabrini, E.; Donà, A.; Falqui, A.; Diaz-Fernandez, Y.; Milanese, C.; Taglietti, A.; Pallavicini, P. *Chem.−Eur. J.* **2012**, *18*, 9381−9390.
(85) Ye, X.; Zheng, C.; Chen, J.; Gao, Y.; Murray, C. B. *Nano Lett.* **2013**, *13*, 765−771.
(86) Ye, X.; Jin, L.; Caglayan, H.; Chen, J.; Xing, G.; Zheng, C.; Doan-Nguyen, V.; Kang, Y.; Engheta, N.; Kagan, C. R.; Murray, C. B. *ACS Nano* **2012**, *6*, 2804−2817.
(87) Kanicky, J. R.; Shah, D. O. *J. Colloid Interface Sci.* **2002**, *256*, 201−207.
(88) Wang, D.; Nap, R. J.; Lagzi, I.; Kowalczyk, B.; Han, S.; Grzybowski, B. A.; Szleifer, I. *J. Am. Chem. Soc.* **2011**, *133*, 2192−2197.
(89) Ye, X.; Gao, Y.; Chen, J.; Reifsnyder, D. C.; Zheng, C.; Murray, C. B. *Nano Lett.* **2013**, *13*, 2163−2171.
(90) Zheng, H.; Smith, R. K.; Jun, Y.-W.; Kisielowski, C.; Dahmen, U.; Alivisatos, A. P. *Science* **2009**, *324*, 1309−1312.